DOI: 10.13009/EUCASS2017-292

On the origin and development of the streaks in flat plate supersonic boundary layer

*Alexander Kosinov***, Nikolai Semionov*, Gleb Kolosov*,*
Alexandra Panina, Yury Yermolaev*, Aleksey Yatskikh ****
**Khristianovich Institute of Theoretical and Applied Mechanics SB RAS*
Institutskaya st., 4/1, Novosibirsk, 630090 Russia
***Novosibirsk State University*
Pirogova st., 2, Novosibirsk, 630090, Russia

Abstract
Origin of the streaks are examined in flat plate boundary layer at Mach 2 and 2.5. They arise due to the interaction of the weak shock waves with flow in vicinity of the flat plate leading edge. The process is accompanied by significant increasing of the pulsation amplitudes in the boundary layer. The effect for the sharp leading edge is not so visible. The case of flat plate with blunted leading edge of 0.6 mm in radius is tested here. Results concerning the influence of small angles of attack of the flat plate is also considered in the paper.

1. Introduction

The transition mechanisms in a supersonic boundary layer are largely dependent on the level of disturbances in the free flow. For example, conventional supersonic wind tunnels have the measurable level of acoustic pulsations in the test section [1, 2], which leads to the early laminar-turbulent transition. The effect of acoustic pulsations on the turbulence origin in a supersonic boundary layer was mainly investigated for the flat plates [3, 4].
Experimental studies of the transition onset in the supersonic boundary layers carried out at ITAM SB RAS over the past five years have made it possible to establish a special scenario for a laminar-turbulent transition arising due to the interaction of stationary weak shock waves with the flow in the vicinity of the attachment line at the leading edges of the models. This scenario introduces its own peculiarities in the process of turbulence in the supersonic boundary layer, which was not previously described and has not been investigated in detail. Such steady-state disturbances in supersonic flow of the T-325 wind tunnel were detected during the installation of models in the region of windows in test section for optical flow visualization with the simultaneous measurement of flow parameters in the boundary layer of a delta wing by a hot-wire anemometer or a Pitot tube [5]. In experiments [6-8], it was possible to simulate this situation using two-dimensional roughness elements of controlled height and width placed on the lateral surface of the walls of the test section or nozzle. It was found that these stationary disturbances, observed during shadow visualization in the form of Mach waves, are generated even by a very small protrusion or ledge of the optical windows on the side wall of the wind tunnel (which in fact always existed). In model experiments, the height of the two-dimensional surface roughness was less than 0.01 mm, and its width (along the stream) was about one thickness of the turbulent boundary layer on the walls of the test section. Hot-wire measurements of the artificially supersonic flow perturbed in this manner performed in the test section made it possible to establish that the shape of the stationary perturbation (in form of the normalized mean mass flow) resembles the N-wave [7–11]. From shadow visualization, it possible to observe a pair of Mach waves generated by the front and back edges of a 2D sticker on the surface of the T-325 nozzle. By these perturbations, we mean paired weak shock waves, and we regard each of them as a single weak shock wave. We have studied simple cases of the effect of single and paired weak shock waves of a fixed intensity on the boundary layers in a supersonic flow. Typical case is when a flat oblique shock fell from the side wall to the leading edge of the models [7-11]. Experiments have shown that in these cases the transition in the boundary layer of models is not described in the framework of traditional concepts. High-intensity stationary streaks were found out in the boundary layer downstream. These high-intensity stationary perturbations arise in the vicinity of the leading edge and almost do not decay downstream. It is determined that they substantially increase the skin friction near the leading edge, during the laminar-turbulent transition, and also continue to exist in turbulent flow. The intensity of the generated perturbations does not have a monotonous dependence with bluntness radius increasing of the leading edge of the models. For

DOI: 10.13009/EUCASS2017-292

studies in T-325 (with a rectangular test section), it is possible to determine the mechanism of generation of such perturbations in the boundary layer. We assume that such a mechanism can be connected both with the interaction of the incident weak shock wave with the boundary layer on the attachment line and with the bow shock.
So it is possible to resume that in some cases in addition to acoustic pulsations there are the quasi-stationary perturbations in the form of weak shock waves in the test section of the wind tunnel that can affect for transition onset too. We have reported about the abnormally high levels of mass flow fluctuations in the boundary layer of the flat delta wing, which achieved up to 20% of the local value of the mass flow [7]. The cause of these high-intensity disturbances could be attributed either to the impact of external weak shock wave on the boundary layer along the attachment line of the leading edge of the delta wing, or with its interaction with bow shock. To test this in [9] it was experimentally investigated the excitation of disturbances by weak shock waves and its influence on the laminar-turbulent transition process in the boundary layer on attachment line of swept cylinder with subsonic leading edge at Mach 2.5. The effect of the interaction of the incident weak shock wave with the bow shock should be checked more in details. We have always detected streaks in the boundary layer of flat delta wing with subsonic, sonic or supersonic leading edges.
The origin of the streaks in flat plate boundary layer with small pluntness of the leading edge at Mach 2 and 2.5 is considered in the paper.

2. Set-up of the experiments

The experiments were conducted in T-325 supersonic wind tunnel of the ITAM SB RAS at Mach 2 and 2.5. We used the flat plates with slightly blunted leading edge (bluntness radius was 0.3 mm or 0.6 mm). Flat plate with the leading edge bluntness of 0.6 mm was placed under different angles of attack $\alpha = 0°, -0.5°, -1°$. Figure 1 show the typical experimental set-up. Here 1 and 2 is pair of the weak shock waves, 3 is control section to checking the initial disturbance distribution, 4 and 5 is trajectory of the streaks in the boundary layer. The coordinate $z = 0$ corresponds to the centreline along the width of the model, $x = 0$ corresponded to the leading edge. To create a pair of weak shock waves a 2D sticker is glued on the sidewall surface of the test section upstream of the model that is similar to [7, 9]. The sticker had about 140 mm in length, about 7 mm in width and about 0.13 mm in thickness. The distance L was different for Mach 2 and 2.5 and is chosen so that the N-wave falls approximately to the central area of the model. To measure the supersonic flow characteristics, the constant temperature anemometer (CTA) with single tungsten wire of 10 microns in diameter and 1.5 mm in length is used. To measure the pressure distribution over the model surface a Pitot tube is applied. With the help of the traversing gear the probe was moved in *x, y, z* directions. Accuracy of sensor in *x, z* directions was 0.1 mm, and 0.01 mm for *y*. At the probe movement along the transverse coordinate, the flow pulsation measurements were carried out at x = const and y = const. The wire overheat ratio was installed about 0.8, so the measured disturbances consisted from mass flow pulsations on 95% [14]. The mean voltage E of output signal from the HWA was measured with a digital voltmeter Agilent 34401A. Pulsations of output signal from the HWA was digitalized by 12-bit analog-to-digital converter (ADC) with a sampling frequency of 750 kHz and recorded to the computer memory. Four time traces of 65536 points in length of each were measured for the all probe positions.

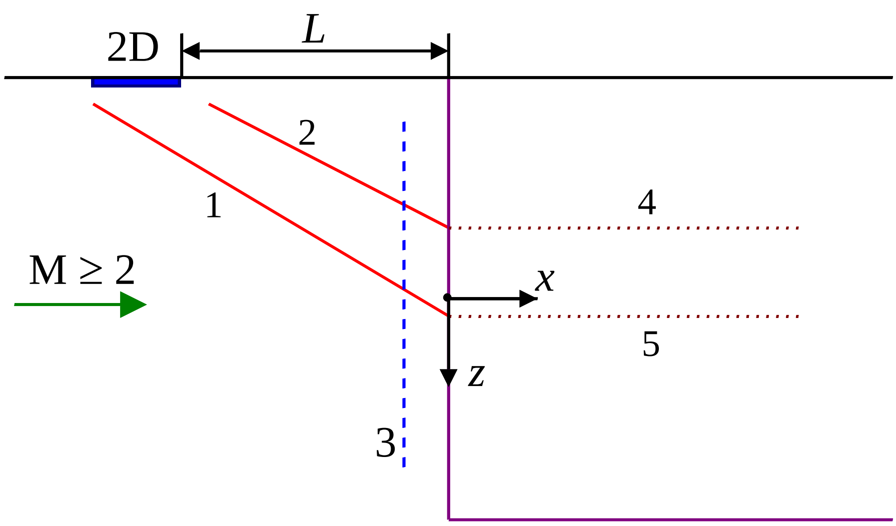

Figure 1: Set-up of the experiments

DOI: 10.13009/EUCASS2017-292

3. Data processing

To determine the character of natural disturbance evolution in the boundary layer, a statistical approach was used, which allowed one to define the linear and nonlinear pulsation development [15].
To determine the mean flow distortion, the relative change of the average mass flow in the spanwise direction is used. The procedure can be obtained by using the relation between the mean voltage output from the anemometer and the mean mass flow [14]:

$$2\frac{\Delta E}{E} \approx n\frac{\Delta(\rho U)}{\rho U}. \tag{1}$$

Amplitude–frequency spectra of disturbances is defined from following procedure

$$m'_f = \frac{\sqrt{2}}{N} \cdot \left| \sum_{l}^{N} m'(t_l) \cdot e^{-i \cdot 2\pi \cdot f \cdot t_l} \right|. \tag{2}$$

The mass flow pulsation *m'* measured by hot-wire was normalized on the local value of the mean mass flow.

4. Results

Pulsations of the supersonic flow in the test section of the T-325 have a normal distribution for the amplitude that does not correspond to their interaction in a free flow. Generated by two-dimensional sticker, the disturbances in the free flow have local non-linear properties, which are characterized by significant deviation of the amplitude distribution from the normal probability density. It was checked by the hot-wire measurements of the spanwise pulsation distribution in the free flow. As for the mean mass flow distribution, the relative value reminds well-known N-wave.

4.1 Flat plate with leading edge bluntness of 0.2 mm at Mach 2

The results of investigation of the radiation field from the two-dimensional sticker placed on the sidewall of the test section of the wind tunnel at Mach 2 and unit Reynolds number 8.3×10^6 m^{-1} are shown in Figures 2–4. The measurements are made in the free flow at the distance $x = -10$ mm i.e. upstream from the leading edge. The distance (L – 10 mm) from the left edge of the sticker to the measurement section was 148 mm. The results of the measurements presented in Figure 2 are functions of mass flow pulsations $\langle m' \rangle$ and the normalized mean mass flow ρU over the transversal *z*–coordinate. Transversal mean flow distortion at Mach 2 is similar to that of N-wave. Almost linear growth of the mean mass flow in the middle part is replaced by a segment of weak stabilization of the growth of the mean mass flow. Such stabilization was previously observed in a stronger form for stickers of greater width [7] at Mach 2.5. Obviously, in order to obtain a linear increase of the mean mass flow in the middle part of the "N-wave" at M = 2, it is necessary to reduce the width of the sticker. From pulsation distribution shown in Figure 2, it follows that the conditions for the undisturbed flow correspond to the data for $z > -2.5$ mm. This region determines the level of disturbances in the test section of T-325 and the natural homogeneity of the mean flow. To calculate the relative mass flow value, these data were used to refine the calibration coefficients of the hot-wire probe. As can be seen from Figure 2, a decrease in the relative mass flow value by approximately 1% for the flow at $z < -20$ mm in comparison with data for $z > -2.5$ mm is obtained. The most probable cause of this is associated with a slight decreasing in the temperature of the cold wire (cold resistance), which follows from the wind tunnel data regarding to the initial parameters of the mean flow.
Statistical analysis of the data measured in the free stream at Mach 2 is performed in four regions with respect to *z*: 1 – the free flow region unperturbed by Mach waves; 2 – the region of the passage of a weak shock wave from the downstream (right) edge of the sticker; 3 – the region of the oncoming stream located between the Mach waves; 4 – the area of passage of a weak shock wave from the upstream (left) edge of the sticker. These areas are shown in Figure 2 by arrows in the total pulsation distribution over *z*.

DOI: 10.13009/EUCASS2017-292

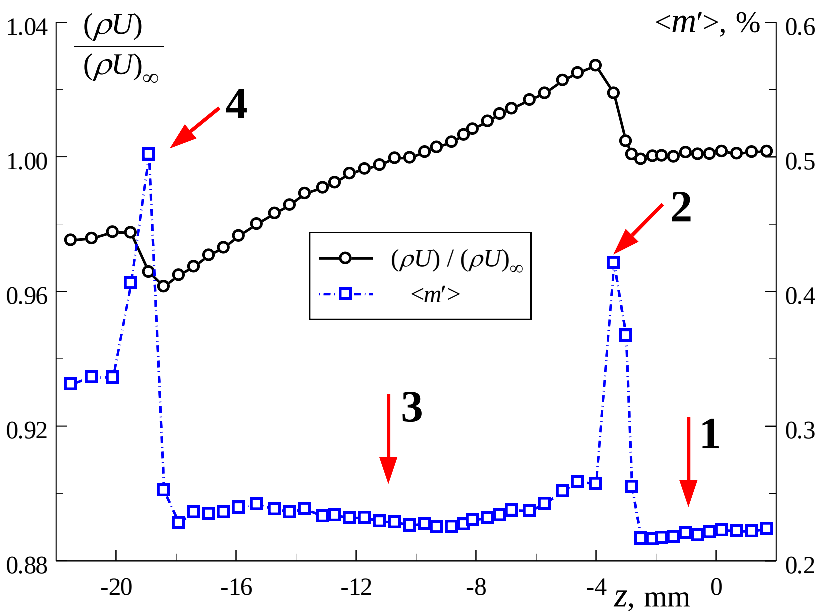

Figure 2: Mass flow pulsations <*m*′> and the normalized mean mass flow ρU distributions over *z*–coordinate in free flow at M = 2. 2D sticker: d ≈ 7 mm, h = 130 μm, L–10 mm = 148 mm

The distributions of the probability density for various values of the transverse coordinate *z* are shown in Figure 3. In the region of the unperturbed incident flow, the histograms coincide with the Gaussian function, to within an error of measurement. An analogous situation is observed in region 3. In the regions 2 and 3 there is a passage of Mach waves, the obtained probability density distributions deviate from the normal law. The greatest deviation is fixed in region 4, where the total integral pulsations are maximal.

Amplitude-frequency perturbation spectra are shown in Figure 4. Here the data are presented for the regions of passages for the Mach waves of the measuring sections (regions 2 and 4). As can be seen from Figure 4, with the passage of a weak shock wave in the incoming stream, low-frequency pulsations with frequencies up to 10 kHz increase. The greatest increase in the disturbances is observed from the Mach wave emanating from the left edge of the sticker.

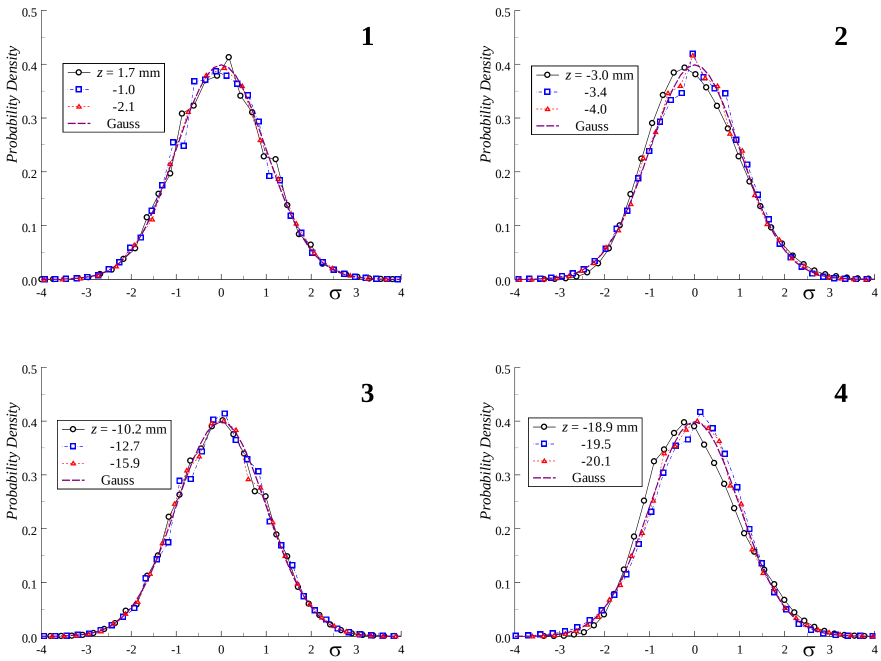

DOI: 10.13009/EUCASS2017-292

Figure 3: Pulsation probability density in typical probe positions at Mach 2

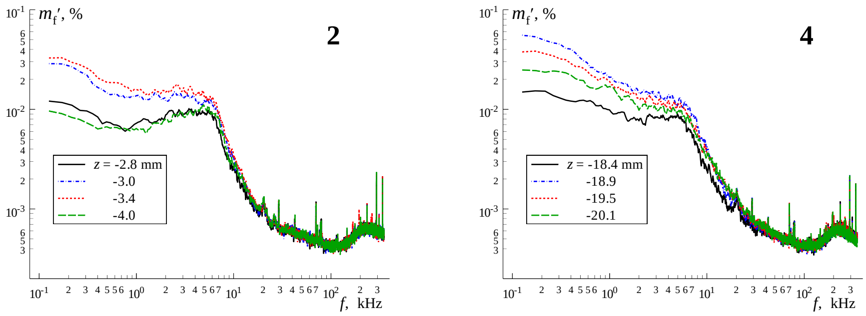

Figure 4: Pulsation amplitude-frequency spectra in typical probe positions at Mach 2

4.2 Flat plate with leading edge bluntness of 0.2 mm at Mach 2.5

Similar to previous section results obtained at M = 2.5 and unit Reynolds number 8.3×10^6 m^{-1} from the same 2D sticker are shown in Figures 5-7.

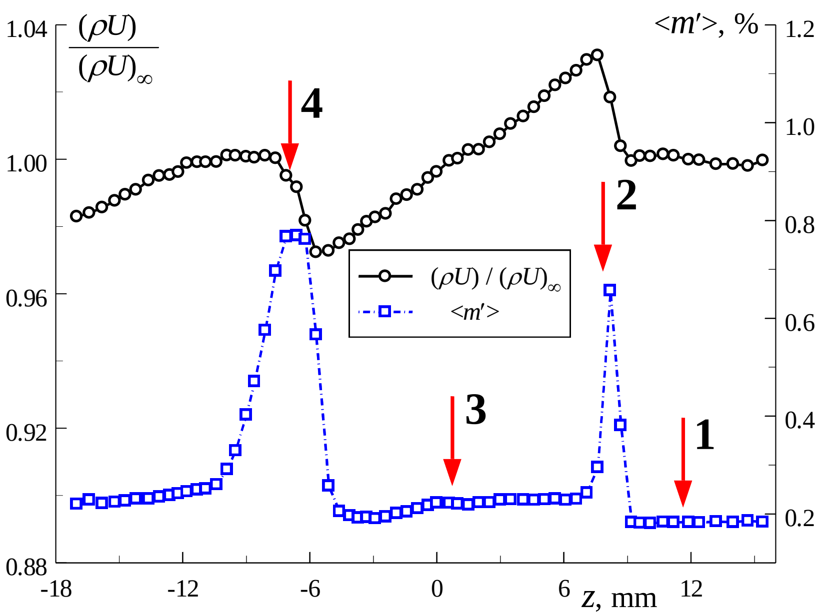

Figure 5: Mass flow pulsations <m'> and the normalized mean mass flow ρU distributions over z in the free flow at M = 2.5. 2D sticker: d ≈ 7 mm, h = 130 μm, L–10 mm = 207 mm

The measurements are made in the free flow at the distance x = –10 mm i.e. upstream from the leading edge. The distance (L–10 mm) from the left edge of the sticker to the measurement section was 207 mm. The results of the measurements presented in Figure 5 are functions of mass flow pulsations <m'> and the normalized mean mass flow ρU over the transversal z–coordinate. Transversal mean flow distortion at Mach 2.5 as well as at Mach 2 is similar to N-wave too. Almost linear growth of the mean mass flow in the middle part is detected. From pulsation distribution shown in Figure 5, it follows that the conditions for the undisturbed flow correspond to the data for z > –9 mm. This region determines the level of disturbances in the test section of T-325 and the natural homogeneity of the mean flow. To calculate the relative mass flow value, these data were used to refine the calibration coefficients of the hot-wire probe.
Statistical analysis of the data measured in the free stream at Mach 2.5 is also performed in four regions with respect to z: 1 – the free flow region unperturbed by Mach waves; 2 – the region of the passage of a weak shock wave from the downstream (right) edge of the sticker; 3 – the region of the oncoming stream located between the Mach waves;

DOI: 10.13009/EUCASS2017-292

4 – the area of passage of a weak shock wave from the upstream (left) edge of the sticker. These areas are shown in Figure 5 by arrows in the total pulsation distribution over *z*.
The distributions of the probability density for various values of the transverse coordinate *z* are shown in Figure 6. In the region of the unperturbed incident flow, the histograms coincide with the Gaussian function, within an error of measurement. An analogous situation is observed in region 3. In the regions 2 and 3 there is a passage of Mach waves, the obtained probability density distributions deviate from the normal law. The greatest deviation is fixed in region 4, where the total integral pulsations are maximal.
Amplitude-frequency perturbation spectra are shown in Figure 7. Here data are presented for the regions of passage of the Mach waves of the measuring section (regions 2 and 4). As can be seen from Figure 7, with the passage of a weak shock wave in the incoming stream, low-frequency pulsations with frequencies up to 10 kHz increase. The greatest increase in the disturbances is observed from the Mach wave emanating from the left edge of the sticker.

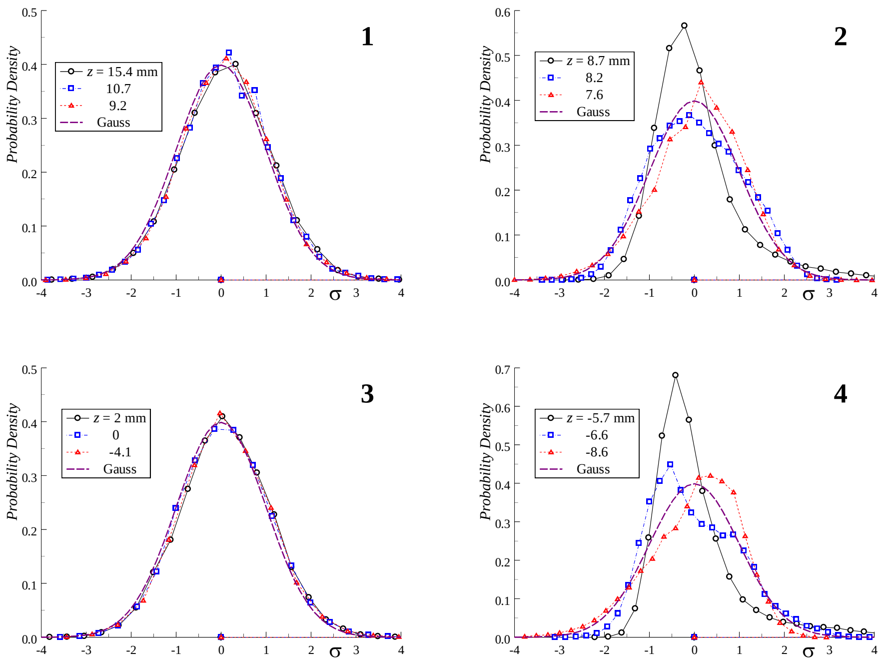

Figure 6: Pulsation probability density in typical probe positions at Mach 2.5

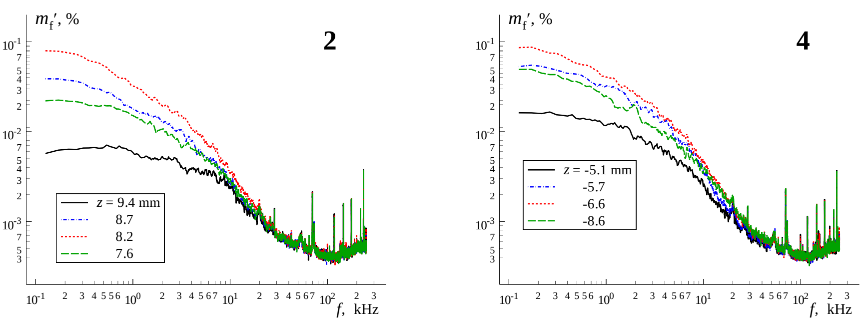

Figure 7: Pulsation amplitude-frequency spectra in typical probe positions at Mach 2.5

4.3 Flat plate with leading edge bluntness of 0.2 mm at Mach 2. Angle of attack influence

The results of the hot-wire measurements in the flat plate boundary layer were similar to results published in [7]. The pulsation amplitude reaches approximately 8-10%. Distortion of the mean flow in the spanwise direction indicates the existence of a pair of vortices in the boundary layer. As an indicator of the skin friction Pitot tube measurements over the flat plate surface is used. Relevant pressure distributions were obtained. It is found out that at the downstream distance up to 100 mm from the leading edge, the boundary layer remains laminar, despite of the existence of stationary vortices and their significant influence to the skin friction. Spanwise scale of the stationary perturbations generated by the external weak shock waves almost does not changed downstream in boundary layer.

DOI: 10.13009/EUCASS2017-292

The distributions of mass flow pulsations <*m*'> and the normalized mean mass flow in the boundary layer as a function of the transverse coordinate *z* at the attack angle α from 0° to 1° are shown in Figure 8. When Mach waves fall the leading edge of the flat plate, the regions of the disturbed flow are found in the boundary layer above the model surface. For mean flow and pulsations, the width of the region was about 20 mm from $z = -15$ mm to $z = 5$ mm. It's value agrees well with the results shown in Figure 2. The region of the disturbed flow by pulsations contains two intense peaks, the amplitude of which reaches approximately 5% (see Figure 9).

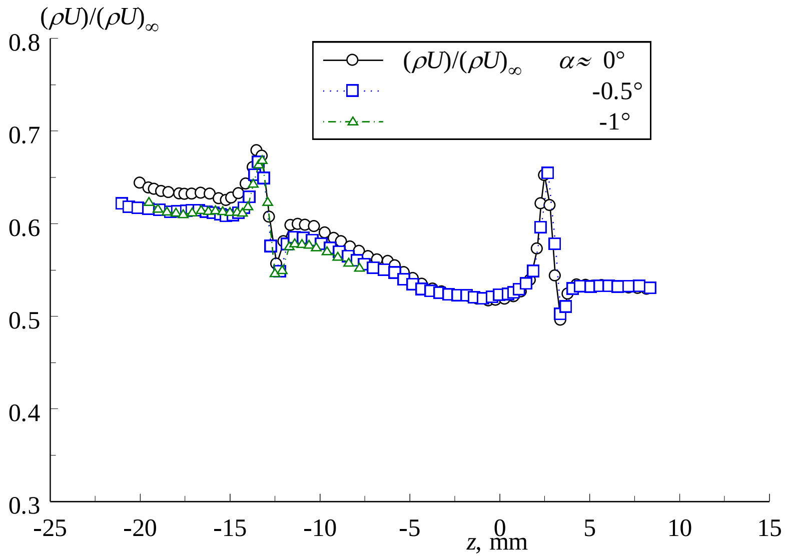

Figure 8: Comparison of the distributions of the normalized mean mass flow ρU in the boundary layer as a function of the transverse coordinate *z* for different angles of attack at Mach 2, Re_1=8.3×10^6 m^{-1}. 2D sticker: d ≈ 7 mm, h = 130 μm, L = 158 mm

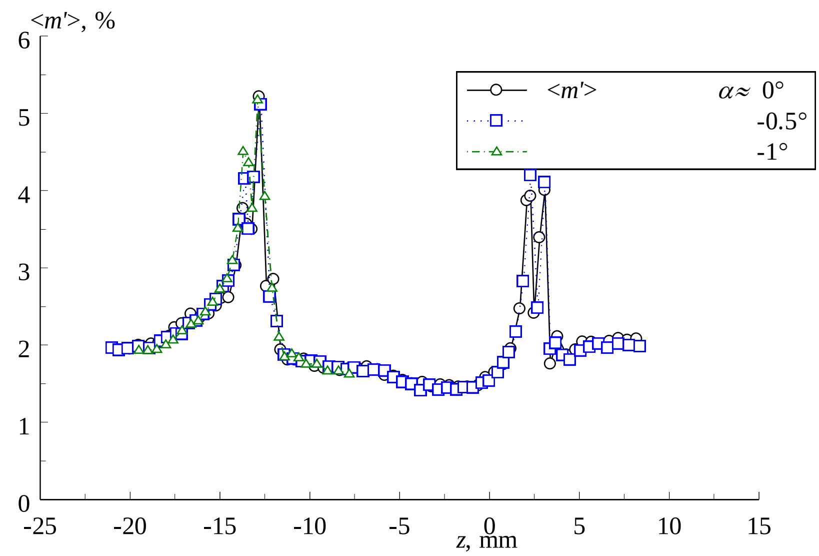

Figure 9: Comparison of the distributions of the mass flow pulsations <*m*'> in the boundary layer as a function of the transverse coordinate *z* for different angles of attack at Mach 2, Re_1=8.3×10^6 m^{-1}. 2D sticker: d ≈ 7 mm, h = 130 μm, L = 158 mm

DOI: 10.13009/EUCASS2017-292

The data are given without correction of the change in the overheat loading of the hot-wire during the experiment. Since the change in the total temperature during the measurements was insignificant (no more than 1.5 K), it is difficult to expect that the correction of these data will lead to a change in the distributions. On this basis, we can conclude that the model prepared for these experiments is not an ideally flat surface, which led to a significant difference in the data at the edges of the distribution ($z < –16$ mm and $z > 4$ mm). However, this did not affect the main results:

1. The observed distributions of the normalized mean mass flow are typical for a vortex. There are two such vortices in the boundary layer, one from each incident weak shock wave.
2. Apparently, a characteristic feature of the vortex structure of stationary disturbances generated in the boundary layer is the presence of two maxima in the distributions of mass flow pulsations in the region of vortices corresponding to the maximum gradients of the mean mass flow along the transverse coordinate.

Since the results for $\alpha = 0°$ and $–0.5°$ were practically the same, in experiments at $\alpha = –1°$ measurements were made only in the region of influence of the trailing edge of the "N-wave". Comparison of the distributions of the normalized mean mass flow and mass flow pulsations $<m'>$ in the boundary layer as a function of the transverse coordinate z for different angles of attack are shown in Figure 8 and 9 respectively. It was obtained that a small change in the angle of attack does not lead to any significant changes in the character of the obtained distributions of the normalized mean mass flow and mass flow pulsations in the boundary layer.

4.4 Flat plate with leading edge bluntness of 0.6 mm at Mach 2. Pitot tube measurements

In Figure 10 shows the distribution of the Pitot pressure on the model surface in the region of the action of a pair of weak shock waves generated by 2D sticker (thickness – 130 microns) on the test section wall at $x = 60$ and 100 mm. These results show the vortex structure of the generated perturbations in the boundary layer and their non-spreading in the transverse direction with increasing coordinate x. The intensities of the streaks generated by a pair of weak shock waves in the boundary layer are different. The wave 1 (see Figure 1) exerts a stronger increase in the surface friction in the region of action in comparison with the wave 2.

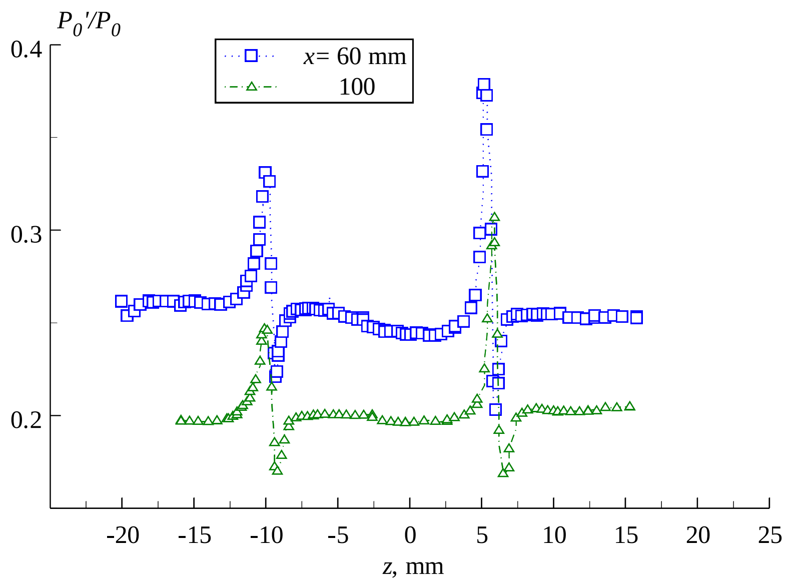

Figure 10: Pitot pressure distributions at Mach 2 in boundary layer; flat plate with bluntness of 0.6 mm; $Re_1 = 8.2 \times 10^6$ m^{-1}; 2D sticker: d = 6 mm; h = 130 μm

It was found that in the measurement region from 60 mm to 100 mm downstream the flow in the boundary layer remains laminar, despite the presence of stationary vortices. These data confirm one of the features of the generated perturbations evolution noted in [6, 7, 12, 13]: they are not spreading along the transverse coordinate downstream.
Figure 11 shows the results of measurements in the boundary layer of the flat plate by hot-wire. It can be seen that the results of pitot pressure measurements and hot-wire measurements are consistent with each other.

DOI: 10.13009/EUCASS2017-292

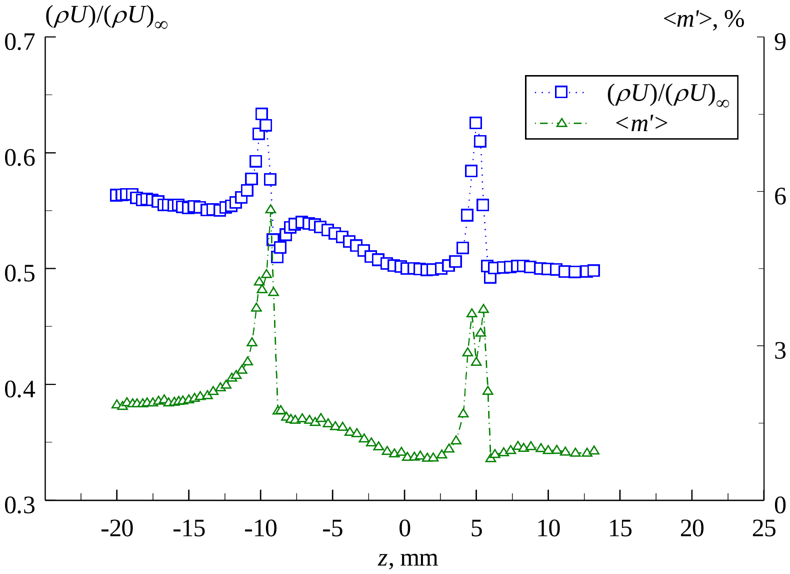

Figure 11: Data obtained by hot-wire in boundary layer at Mach 2; flat plate with bluntness of 0.6 mm; x = 60 mm; $Re_1 = 8.3\times10^6$ m^{-1}; 2D sticker: d = 6 mm; h = 130 μm

5. Acknowledgement

The work was supported by Russian Scientific Foundation (grant number 17-19-01289).

References

[1] Laufer J. 1961. Aerodynamic noise in supersonic wind tunnels *J. Aerospace Sci*. 28(9): 685-692,

[2] Kendall J.M. 1975. Wind tunnel experiments relating to supersonic and hypersonic boundary-layer transition. *AIAA J*, 13(3): 290-299.

[3] Kosinov A.D., Maslov A.A., Semionov N.V. 1997. An experimental study of generation of unstable disturbances on the leading edge of a plate at M = 2. *J. AMTP*. 38(1): 45-51.

[4] Schneider S.P. 2001. Effects of high-speed tunnel noise on laminar-turbulent transition. *J. Spacecraft and Rockets*. 38(3): 323-333.

[5] Vaganov A.V., Ermolaev Yu.G., Kosinov A.D., Semionov N.V., and Shalaev V.I. 2013. Experimental study of flow structure and transition in the boundary layer of a delta wing with blunted leading edges at Mach numbers 2, 2.5, and 4. *Proc. of Moscow Institute of Physics and Technology*, 5(3): 164−173. (in Russian).

[6] Vaganov A.V., Ermolaev Yu.G., Kolosov G.L., Kosinov A.D., Panina A.V., and Semionov N.V. 2014. Action of incident Mach wave on the field of pulsations in boundary layer of a planar delta wing. *Vestnik NGU, ser. Fizika,, 9(1)*: 29−38, (in Russian).

[7] Vaganov A.V.; Ermolaev Yu G.; Kolosov G.L.; Kosiniv A.D., Panina A.V., Semionov N.V. 2016. Impact of incident Mach wave on supersonic boundary layer. *Thermophysics and Aeromechanics.* 23(1): 43-48.

[8] Yatskih A.A., Kolosov G.L., Kosinov A.D., Yermolaev Yu.G., Panina A.V., Semionov N.V. 2016. Experimental study of the effect of a couple weak shock waves on a laminar-turbulent transition on the attachment line of a swept cylinder. *Vestnik NGU, ser. Fizika*, 11(2): 28–36. (in Russian).

[9] Yermolaev Yu.G., Yatskih A.A., Kosinov A.D., Semionov N.V., Kolosov G.L. and Panina A.V. 2016. Experimental study of the effects of couple weak waves on laminar-turbulent transition on attachment-line of a swept cylinder. In: *International Conference on the Methods of Aerophysical Research (ICMAR 2016)* AIP Conf. Proc. 1770, 020012-1–020012-8; http://dx.doi.org/10.1063/1.4963935

[10] Kosinov A.D., Yermolaev Yu.G., Kolosov G.L., Panina A.V., Semionov N.V., Yatskih A.A. 2016. To the mechanism of the effect of weak shock waves on a laminar-turbulent transition in a supersonic boundary layer. In: *Proc. of the XXII International Conference "Nonlinear Problems of the Theory of Hydrodynamic Stability and Turbulence"*. (in Russian).

DOI: 10.13009/EUCASS2017-292

[11] *Kosinov A.D., Semionov N.V., Kolosov G.L., Yermolaev Yu.G., Yatskih A.A.* 2016. Excitation of the streaks by weak shock waves in the supersonic boundary layer. In: *24th International Congress of Theoretical and Applied Mechanics (ICTAM 2016)*: 695-696.

[12] Kosinov A.D., Panina A.V., Vaganov A.V. 2015. On the effect of a incident Mach wave on a transition in a supersonic boundary layer. In: *XI All-Russian Congress on Basic Problems of Theoretical and Applied Mechanics*: 1998-2000. (in Russian).

[13] Kosinov A.D., Kolosov G.L., Panina A.V., Semionov N.V. 2015. On the effect of weak shock waves on the pulsations and flow in supersonic boundary layer. In: *11th ERCOFTAC SIG33 Workshop Progress in Transition Modelling and Control*,

[14] Kosinov A.D., Semionov N.V., Yermolaev Yu.G. 1999. Disturbances in test section of T-325 supersonic wind tunnel. *Preprint / Russian Academy of Sciences, Siberian Devision, Institute of Thearetical and Applied Mechanics*. 6-99. Novosibirsk. 24 p.

[15] Kosinov A.D., Semisynov A.I. 2003. Character of evolution of natural disturbances in a supersonic boundary layer on a flat plate. *J. Thermophysics and Aeromechanics*. 10(1): 39-44.